The 72-h WEBT microvariability observation of blazar S5 0716+714 in 2009

Bhatta et al.(2013)

Reporter: Xin Chang (常鑫)
email: cx@mail.ynu.edu.cn
Yunnan University
SWIFAR
2024-03-19

Introduction

1. The international Whole Earth Blazar **Telescope (WEBT)** consortium carried out three days of intensive micro-variability observations of S5 0716+714 from February 23 to 26, 2009.

2. Thirty-six observatories in sixteen countries participated in this continuous monitoring program and twenty of them submitted data for compilation into a continuous light curve.

3. The light curve was analyzed using several techniques including Fourier transform, Wavelet and noise analysis techniques.

4. They obtained an excellent fit to the 72-hour light curve with the synchrotron pulse model.

Observation

Observatories contributing observations to the WEBT campaign.

Zone	Code	Country	Observatory	Longitude	Telescope	Filters
1	AAS	Spain	Agrupacion Obs.	0.73	0.5 m	*R*
1	AVO	Italy	Aosta Valley Obs.	7.36	0.81-m	*RI*
1	MAO	Germany	Michael Adrian Obs.	8.41	1.2-m	*BVRI*
2	AAO	Italy	Armenzano Obs.	12.69	36-cm	*R*
3	TUR	Finland	Tuorla Observatory	22.17	35-cm, 1-m	*R*
3	BEL	Bulgaria	Belogradchik	22.60	60-cm	*BVRI*
3	HANK	Finland	Hankasalmi	26.50	40-cm (RC)	*BVRI*
3	STPET	Russia	St. Petersburg	29.82	40-cm	*R*
3	JAKO	Finland	Jakokoski Obs.	30.00	20-inch	*I R*
4	CRIM	Crimea	Crimean AP Obs.	30.20	2.6, 1.25 m	*R*
5	ABAS	Georgia, FSU	Abastumani Obs.	42.80	0.7-m	*R*
6	ARIES	India	ARIES	71.68	1.04 m	*R*
7	BAO	China	BAO China, Xinglong	114.00	1.0-m	*R*
7	WHO	China	Weihai China	122.00	1-m	*BVRI*
8	LOAO	USA	Mt. Lemmon	249.00	1.0-m	*R*
11	MDM	USA	MDM Kitt Peak	249.00	MDM 1.3 m	*R*
11	SARA	USA	SARA/Kitt Peak	249.00	1.-m	*R*
12	BUO	USA	Butler	273.55	0.96-m	*R*
12	DSO	USA	Dark Sky, North Carolina	278.58	24-inch	*R*
13	BLK	Ireland	Cork	352.00	40-cm	*RGB*

1. This table lists 16 countries with different observing codes, observatory name, telescope longitude, telescope size and filters.

2. The code is the key to the observatories responsible for each data segment on the plot.

Observation

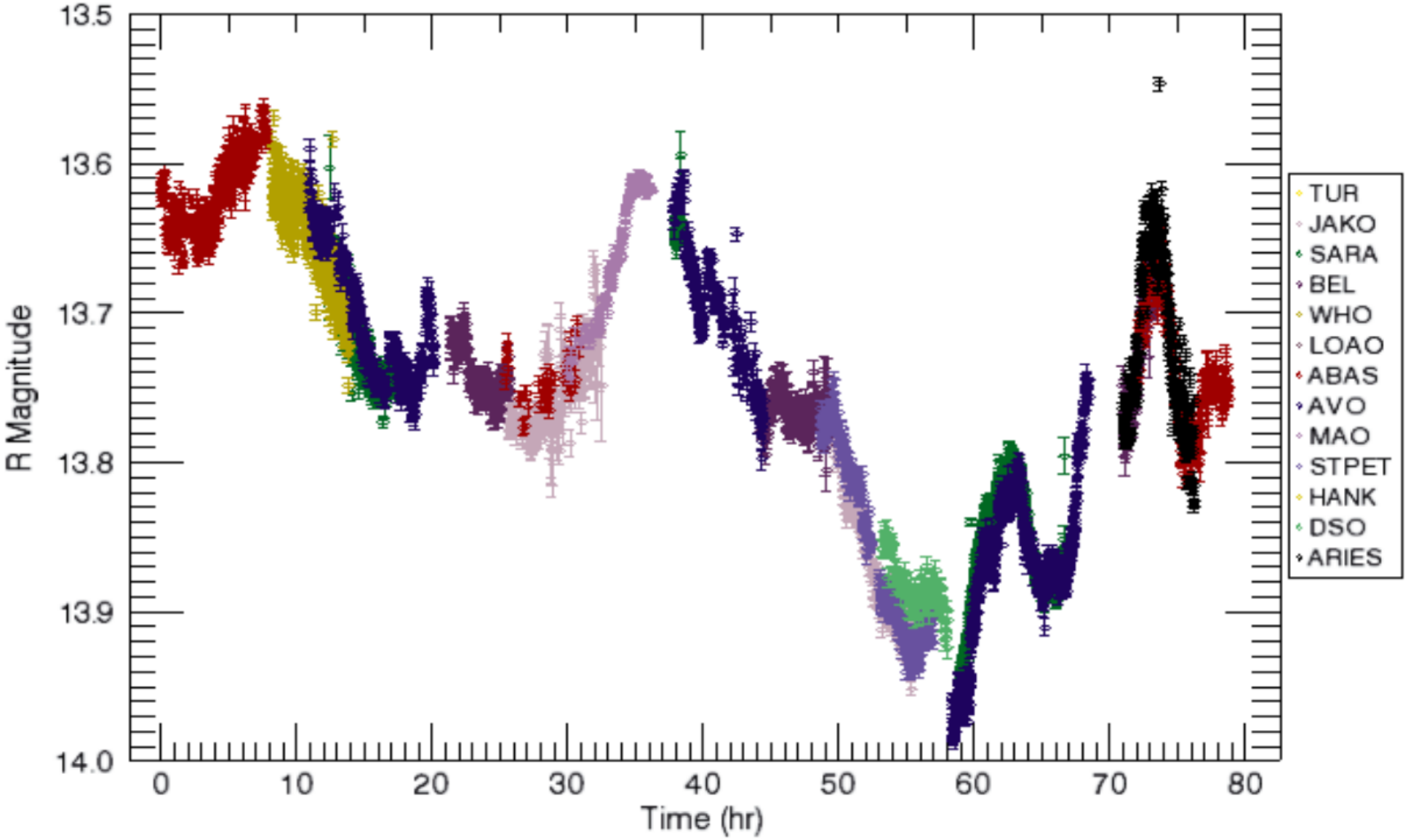

Observation

1. Figure 1 shows the raw observations plotted together.

2. The observations covered the time period from February 23 to 26 in 2009.

3. They made minor zero-point adjustments to obtain a consistent continuous light curve.

4. Exposure times for individual images ranged from 30 s to 120 s depending on the observatory and telescope.

Observation

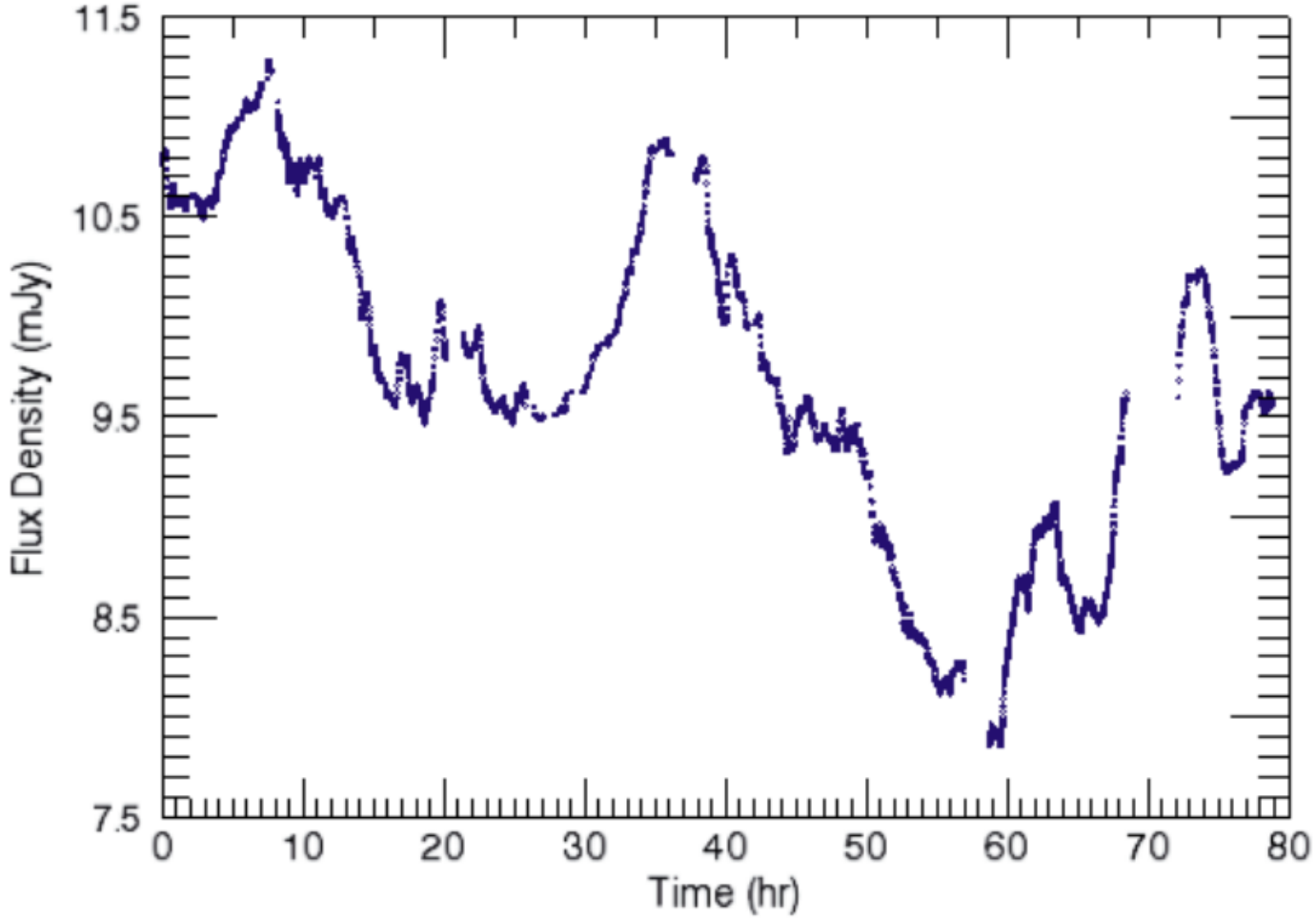

Observation

- Figure 2 shows the complete flux curve.

- **The magnitudes were converted to flux using standard flux conversions for the R filter** as given by Johnson (1966) using a redshift of 0.30 and Galactic absorption of 0.031 mag.

- The total length of the light curve was 78.88 h. They analyzed individual segments of the flux curve to determine the maximum climb and decline rates.

Observation

Seg	Times (h)	Slope (mag/h)	r^2	Npts	Prob.	Rise/Decline
1	3.38–7.01	0.019	0.918	123	5×10^{-7}	Rise
2	13.03–16.54	0.027	0.946	155	5×10^{-7}	Decline
3	18.69–19.84	0.064	0.967	40	1×10^{-6}	Rise
4	29.91–35.76	0.029	0.968	120	1×10^{-6}	Rise
5	38.39–39.91	0.050	0.945	77	5×10^{-7}	Decline
6	49.70–55.30	0.022	0.956	177	5×10^{-7}	Decline
7	58.52–63.10	0.037	0.878	244	5×10^{-7}	Rise
8	63.48–65.20	0.033	0.904	115	5×10^{-7}	Decline
9	66.74–68.46	0.089	0.977	99	5×10^{-7}	Rise
10	72.14–73.60	0.035	0.739	29	1×10^{-6}	Rise
11	74.07–75.63	0.076	0.977	43	1×10^{-6}	Decline
12	75.66–78.17	0.026	0.873	73	5×10^{-7}	Rise

Observation

- Table 2 lists the slopes and correlation coefficients for each climb and decline segments.
- Col. 2: the start and finish time of the segment in hours
- Col. 3: the slope
- Col. 4: the correlation coefficient for each fit
- Col. 5: the number of points.
- Col. 6: the probability of correlation coefficient.
- column 7 denotes whether the slope is a rise or a decline.
- **The results show that** the average decline rate was 0.042 mag/h (standard deviation of 0.022) while the average rise rate was 0.043 with a standard deviation of 0.028. Thus over all, **the rise and decline rates are similar in this segment of light curve.**
- Although the rates are different, the fact that the slopes for the rise and decline are the same agree with the results found by Villata et al. (2000) and Montagni et al. (2006).

Time series analysis

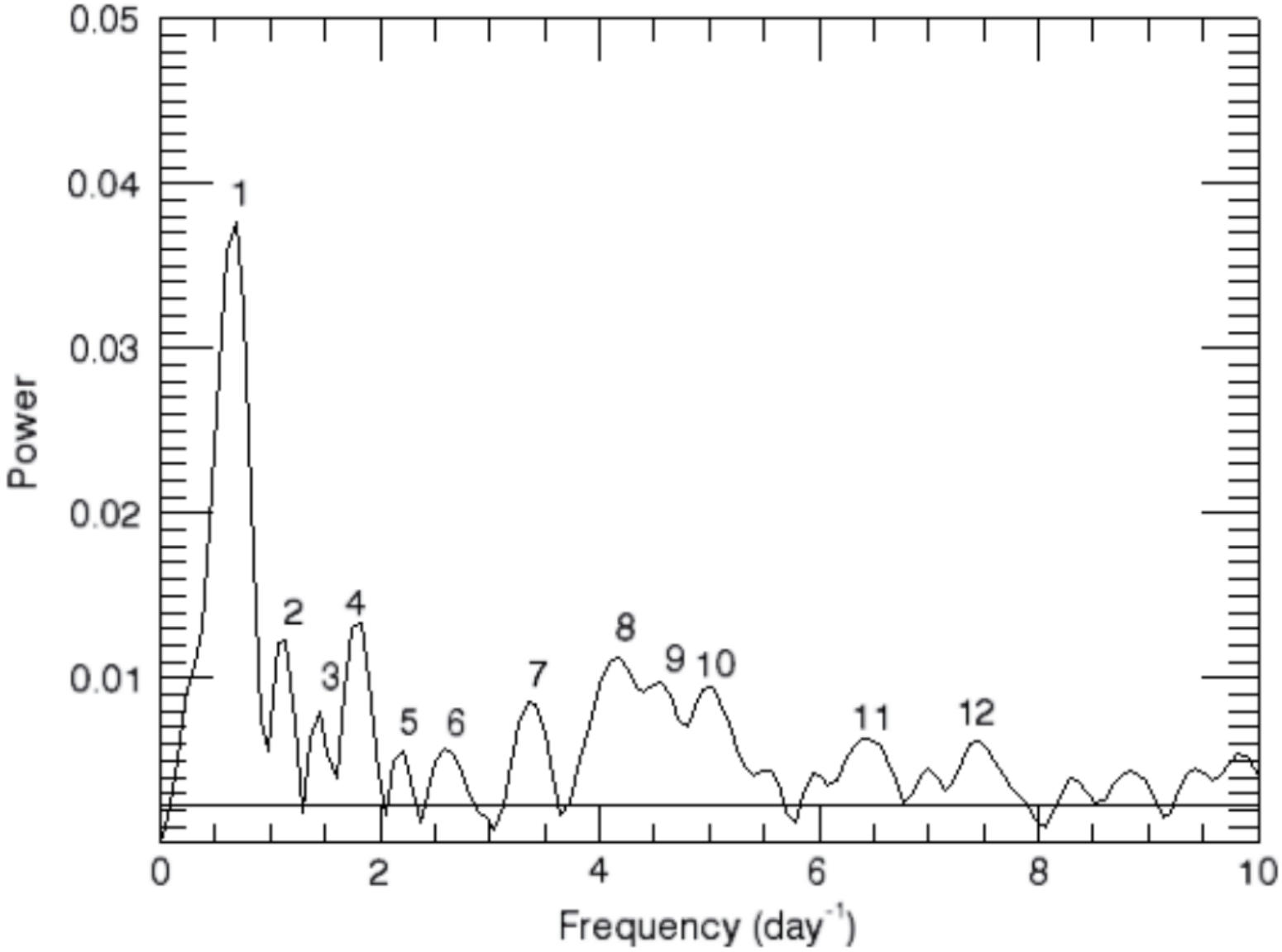

Time series analysis

Number	Frequency (/day)	Power	Timescale in obs. frame (h)	Timescale in rest frame (h)
1	0.60	0.0382	40.00	656.00
2	1.14	0.0122	21.05	345.22
3	1.41	0.0083	17.02	279.13
4	1.82	0.0126	13.19	216.32
5	2.25	0.0052	10.67	174.99
6	2.60	0.0054	9.23	151.37
7	3.40	0.0081	7.06	115.78
8	4.20	0.0121	5.71	93.64
9	4.54	0.0092	5.29	86.76
10	5.00	0.0091	4.80	78.72
11	6.50	0.0063	3.69	60.52
12	7.50	0.0062	3.20	52.48

Time series analysis

- **Fourier transform analysis**
- **They performed Fourier transform analysis on the entire light curve** by using a discrete Fourier transform (DFT) algorithm (Deeming 1975).
- The results of this analysis are shown in Fig. 3 and Table 3.

- **From the results we can see 12 peaks exceeding the horizontal line across the bottom which indicates the peaks exceeding the average power of 100 light curves.**

- Column 4 indicates the time scales of these twelve peaks.
- Column 5 indicates the corresponding time-scales in the rest frame calculated using:

$$\Delta t_{\text{rest}} = \frac{D}{1+z}\Delta t_{\text{obs}} \longleftarrow D = 1/\Gamma\,(1-\beta\cos\theta)$$

Time series analysis

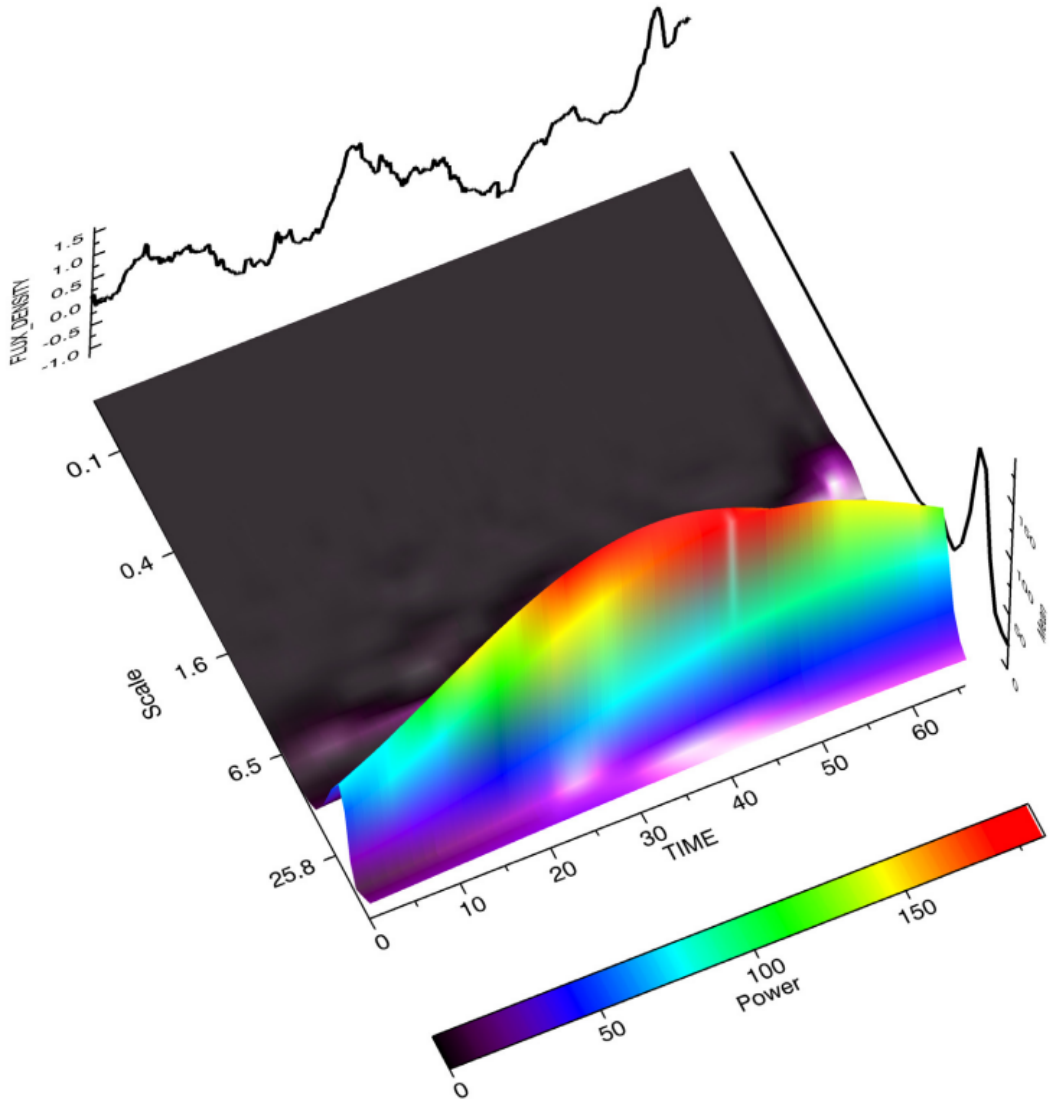

Time series analysis

- Figure 4 shows the result of wavelet transform analysis (Torrence & Compo 1998).

- From this figure we can see the peak is clearly only significant in the center of the data, fitting extremely poorly at the start or end of the light curve.

- **They did not find the periods** at approximately 25 and 73 min in this flux curve seen previously by Gupta et al. (2009). **Thus they could not confirm any of the previously detected periods seen in the S5 0716+714.**

- So, they propose a new model for the interpretation of microvariability.

Modeling the microvariations

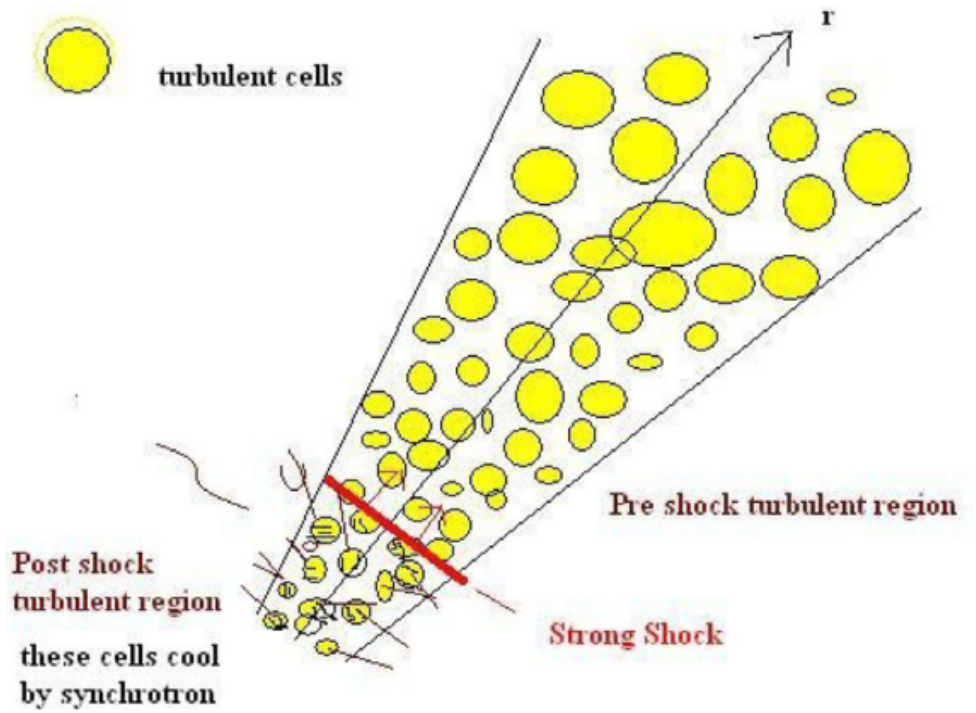

Shock acceleration of electrons and amplification of magnetic fields parallel to the shock front in turbulent cells.

Yields synchrotron cooling in post-shock region from shocked cells.

Modeling the microvariations

- They investigate a model that:

plasma blobs can be generated by magnetic reconnection in the jet. When shocks in the jet interact with plasma blobs, they induce changes in density and temperature, resulting in radiation emission.

The rapid particle acceleration and subsequent cooling by synchrotron emission produces a pulse in the flux curve.

Modeling the microvariations

- **The particle distribution function of this model** given by Ball &Kirk (1992).

$$\frac{\partial N}{\partial t} + \frac{\partial}{\partial \gamma}\left[\left(\frac{\gamma}{t_{\mathrm{acc}}} - \beta_{\mathrm{s}}\gamma^2\right)N\right] + \frac{N}{t_{\mathrm{esc}}} = Q\delta\left(\gamma - \gamma_0\right)$$

with

$$\beta_{\mathrm{s}} = \frac{4}{3}\frac{\sigma_{\mathrm{T}}}{m_{\mathrm{e}}c}\left(\frac{B^2}{2\mu_0}\right)$$

- KRM (Kirk et al. 1998) calculated the particle acceleration in the shock front for various magnetic field orientations and particle densities assuming a plane shock encounters a cylindrical density enhancement.
- **In this model, the ratio of the acceleration time t_{acc} and escape time t_{esc}**, in addition to constraints on the cooling length L **control the pulse shape**.
- **The amplitude is given by the parameter Q and is related to the magnetic field strength B and orientation θ in addition to the enhanced electron density.**

Modeling the microvariations

- **After a number of test solutions, they determined** that for tacc/tesc = 0.5 they get **symmetric pulse shapes similar to what they see in the microvariability curves**. The pulse shape is shown in Fig. 8. **They used this as the standard pulse shape for all subsequent fits.**

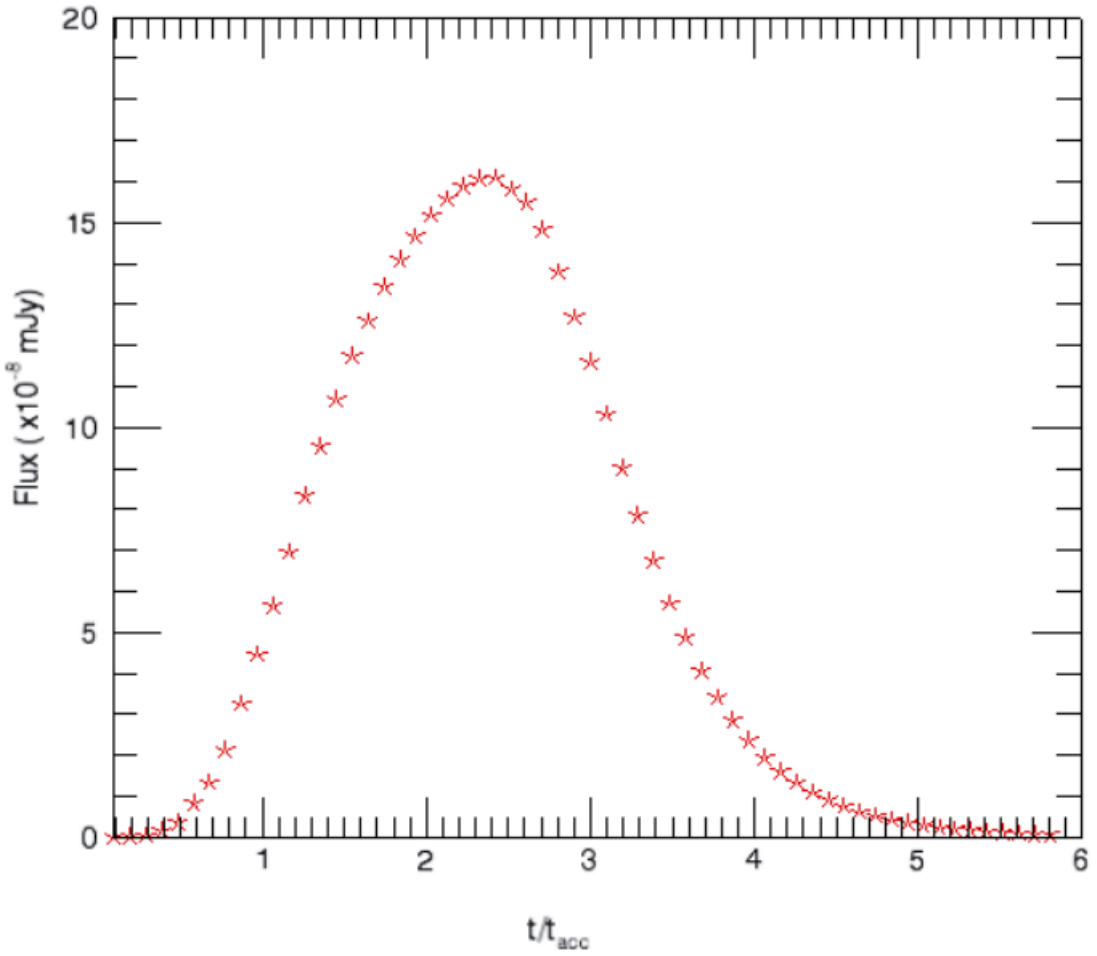

Modeling the microvariations

- **They fit thirty-five pulses to the microvariability curve by varying the width and amplitude of the standard pulse. This Figure shows the light curve fitted with the convolved pulses. The blue points are the smoothed data and the red points are the model.** The fit correlation coefficient is 0.98. Since turbulence is a stochastic process, each microvariability curve is a realization of that stochastic process.

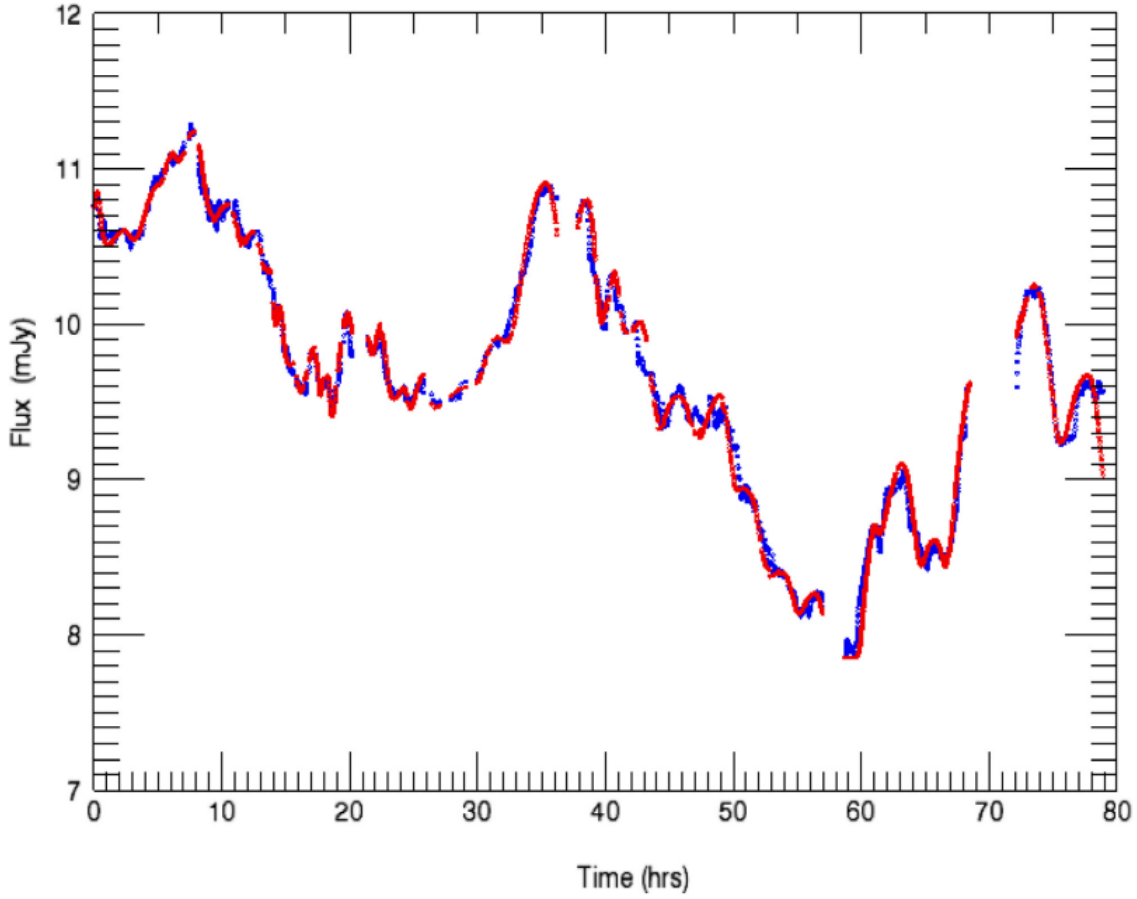

Modeling the microvariations

Pulse	Center (h)	Amp (mJy)	τ_{flare} (h)	N $\times 10^{-5}(s^{-1}\ m^{-3})$	S_{cell} AU	Index
1	0.15	0.57	1.11	4.94	13.18	4
2	2.10	2.74	9.74	23.56	115.35	34
3	5.70	1.27	3.34	10.94	39.54	23
4	7.80	1.47	3.75	12.66	44.49	30
5	8.45	1.24	2.78	10.69	32.95	18
6	10.80	0.14	3.61	1.25	42.84	28
7	10.90	2.39	2.92	20.56	34.60	20
8	13.00	2.34	2.50	20.13	29.66	17
9	14.30	1.29	1.41	11.12	16.80	7
10	14.60	0.19	0.55	1.68	6.59	1
11	15.50	1.69	1.67	14.55	19.77	9
12	17.20	1.94	2.19	16.69	26.03	15
13	18.20	0.72	0.78	6.22	9.22	2
14	19.75	2.04	2.45	17.55	29.00	16
15	21.30	0.57	0.78	4.94	9.22	3

Modeling the microvariations

- The resulting parameters for the pulses used in modeling the light curve are listed in Table 4.
- Column1 is the shot number in time order,
- Column2 is the center time of the pulse.
- Column3 and 4 is the amplitude and width of each of pulse
- Column5 is the electron density enhancement
- Column 6 is the size for the cell

- **The center time is related to the relative location of the cell along the jet.**
- **There is a large range of length/time scales for the turbulent vortices. The smallest vortex timescale is normally associated with the Kolmogorov scale** (where most of the dissipation takes place in non-relativistic plasma) **and the largest length scales are associated with either the size of the plasma jet or the correlation length within the plasma.**

Thanks!